

Optogenetic Tools for Confined Stimulation in Deep Brain Structures

Alexandre Castonguay, Sébastien Thomas, Frédéric Lesage, and Christian Casanova

Abstract

Optogenetics has emerged in the past decade as a technique to modulate brain activity with cell-type specificity and with high temporal resolution. Among the challenges associated with this technique is the difficulty to target a spatially restricted neuron population. Indeed, light absorption and scattering in biological tissues make it difficult to illuminate a minute volume, especially in the deep brain, without the use of optical fibers to guide light. This work describes the design and the in vivo application of a side-firing optical fiber adequate for delivering light to specific regions within a brain subcortical structure.

Key words Deep brain stimulation, Optogenetics, Side-firing optical fiber

1 Introduction

The understanding of brain function ineluctably passes through the investigation of the role played by distinct brain structures. To reveal the function of a specific neuronal structure, one can modulate its activity and measure engendered changes [1]. Classical techniques for neural activity modulation include microelectrical stimulation, drugs delivery, genetic manipulations, or lesions making. While these methods led to clear advances in our understanding of the brain, they are associated with poor spatial resolution, slow kinetics, irreversibility, or collateral effects. Recently, optogenetics emerged as a technique allowing high temporal and spatial resolution control over neural activity [2]. Early investigations using optogenetics have mostly been limited to the neocortex [3–5]. The main reason for this is the limited light penetration in biological tissue [6]. However, to fully understand information processing in the brain, it is also necessary to study the function of deep brain structures. Many groups have shown interest in developing tools for deep brain optogenetic stimulation [7, 8], which has proven to be quite challenging. Indeed, due to the absorption

and scattering of light in the wavelength range used in optogenetics [9], a spatially restricted stimulation of deep brain structures remains difficult without the use of optical fibers to guide light to specific regions.

In this protocol, we present an optogenetic experimental setup that enables the modulation of activity of distinct neural populations in subcortical nuclei of mice expressing ChannelRhodopsin-2. A side-firing optical fiber was developed to shine light in a cylindrical pattern by rotating and translating the fiber around its axis, thus allowing the stimulation of restricted populations of neurons within a thalamic region. Such an approach minimizes the number of fiber penetration needed to probe a given structure, and potentially reduces tissue damage.

Aiming for specific thalamic regions in small animal models such as mice can be quite challenging because of their small size. To assess the spatial extent of optogenetic stimulation, tests were conducted in the visual system, taking advantage of its highly structured network. Indeed, in the visual system of most studied mammals, the organization of the visual field is topographically preserved along the visual pathways through cell distributions and synaptic connections, from the retina to the visual cortex [10]. Here, we used the designed fiber to sequentially stimulate subpopulations of neurons in the lateral geniculate nucleus (LGN), a thalamic structure that receives topographically organized inputs from the retina and projects in an orderly manner to the visual cortex (V1). Effective optogenetic stimulation of subpopulations of neurons in the LGN was validated using intrinsic optical imaging (IOI) of the visual cortex [11].

This protocol is comprised of two main methodological challenges: the development of a precisely rotating side-firing optical fiber and the *in vivo* optogenetic stimulation of a small thalamic region.

2 Materials

2.1 Optical Setup

2.1.1 Side-Firing Optical Fiber

1. One 1 m Optical fiber (SMA connector suggested) with small NA and a core diameter of 200 μm or less to minimize tissue damage (Suggested: M92L01— \varnothing 200 μm , 0.22 NA, SMA-SMA, 1 m, Thorlabs).
2. Fiber stripping tool matching optical fiber size (T01S13, Thorlabs).
3. Glass micropipette.
4. Micropipette beveller (World Precision Instrument, 48000) with sandpapers of various grit sizes (from 10 to 0.3 μm suggested).
5. Electron Beam Physical Vapor Deposition system.

2.1.2 Mechanical System

1. Stepper motor (Matsushita, 55SI-DAYA, precision: 7.5°) and driver (UCN5804B).
2. Two gears with timing belt.
3. Mono-coil tube (HAGITECH, FS-6).
4. Two metal guide tubes (suggested diameter/length: 15 mm/250 mm and 5 mm/300 mm).
5. Two bearings with outer diameter equal to large metal guide inner diameter and an inner diameter equal to small guide tube outer diameter (ABEC-7).

2.1.3 Laser Coupling

1. Optical fiber with same connector, NA and core diameter as in Subheading 2.1.1, step 1.
2. Fiber optic rotary joint (FRJ-v4, Doric).
3. Microscope objective (MV-20x, Newport).
4. Neutral density variable filter (NDC-25C-4M, Thorlabs).
5. Mirror with kinematic mirror mount (KCB1, Thorlabs).
6. X and Y micromanipulators (PT1, Thorlabs).
7. Laser source (DHOM-L-473-50 mW).
8. Optical breadboard (MB1218, Thorlabs).

3 In Vivo Optogenetic Stimulation of Deep Brain Structures

3.1 Reagents

1. Anesthetic (Urethane, 2 g/kg).
2. Local anesthetic (Xylocaine®, 2 %).
3. Skin disinfectant (Povidone-Iodine).
4. Agarose (1 %).
5. Oxygen.

3.2 Equipment

1. Standard surgery tools.
2. Micro drill.
3. Tracheal tube.
4. Needle (24G).
5. Tungsten microelectrode (1–2 MΩ).
6. Electric shaver.

3.3 Setup

1. Side-firing optical fiber setup.
2. Stereotaxic system with stereotaxic arm and electrode holder (Kopf).
3. Electrocardiogram.
4. Feedback-controlled heating pad.

5. Microelectrode amplifier.
6. Imaging data acquisition hardware (Imager 3000, Optical Imaging).
7. Light source (halogen bulb) and fiber optic bundle.
8. Bandpass spectral filters ($\lambda_0 = 545$ nm and 630 ± 15 nm).
9. CCD camera (1M60, Dalsa, Colorado Springs, USA).
10. Lens (Nikon, AF Micro Nikkor, 60 mm, 1:2.8D).

4 Methods

4.1 Optical Setup

4.1.1 Side-Firing Optical Fiber

1. Commercial optical fiber patch cables are usually composed of a core where light propagates, a cladding to maintain light guided in the core and a coating to protect the integrity of the fiber. Cut off the connector from one end of the fiber and remove protective coating to keep only the core and cladding. Using the appropriate fiber-stripping tool, remove cladding 2 cm from the cut optical fiber tip.
2. Insert the bare tip of the optical fiber in a glass micropipette and fix it on the micropipette beveller at an angle of 45° . The glass micropipette will serve as support for the fragile exposed core.
3. Start polishing the silica fiber tip with coarse polishing paper (suggested grit size: $10 \mu\text{m}$) and progressively reduce grit size to have a fine polished surface. If final grit size is smaller than the illumination wavelength, specular reflection will occur on the tip. A $0.3 \mu\text{m}$ grit will lead to such reflection in optogenetic applications.
4. A thin layer (approximately 100 nm) of highly reflective metal, such as chrome, at the fiber tip will ensure an almost 100 % reflection at the fiber tip (Fig. 1a). Electron Beam Physical Vapor Deposition necessitates a fully trained technician to use; therefore the protocol for E-beam usage is skipped here.

4.1.2 Mechanical System

1. The metal guide tube assures that the optical fiber turns on its axis to avoid unbalanced rotation that would damage tissue. Fix the two bearings at each end of the larger metal guide tube, and then insert the smaller guide tube into the bearings (troubleshooting, *see Note 1*). At this point, a small guide tube can freely rotate around its axis, in the center of the large guide tube.
2. To fix the optical fiber in the center of the guide tube, use two cylindrical adaptors with a diameter that fits tightly in the small guide tube and drill a small hole in the center to fit the optical fiber with the cladding. By inserting the fiber in both cylindrical

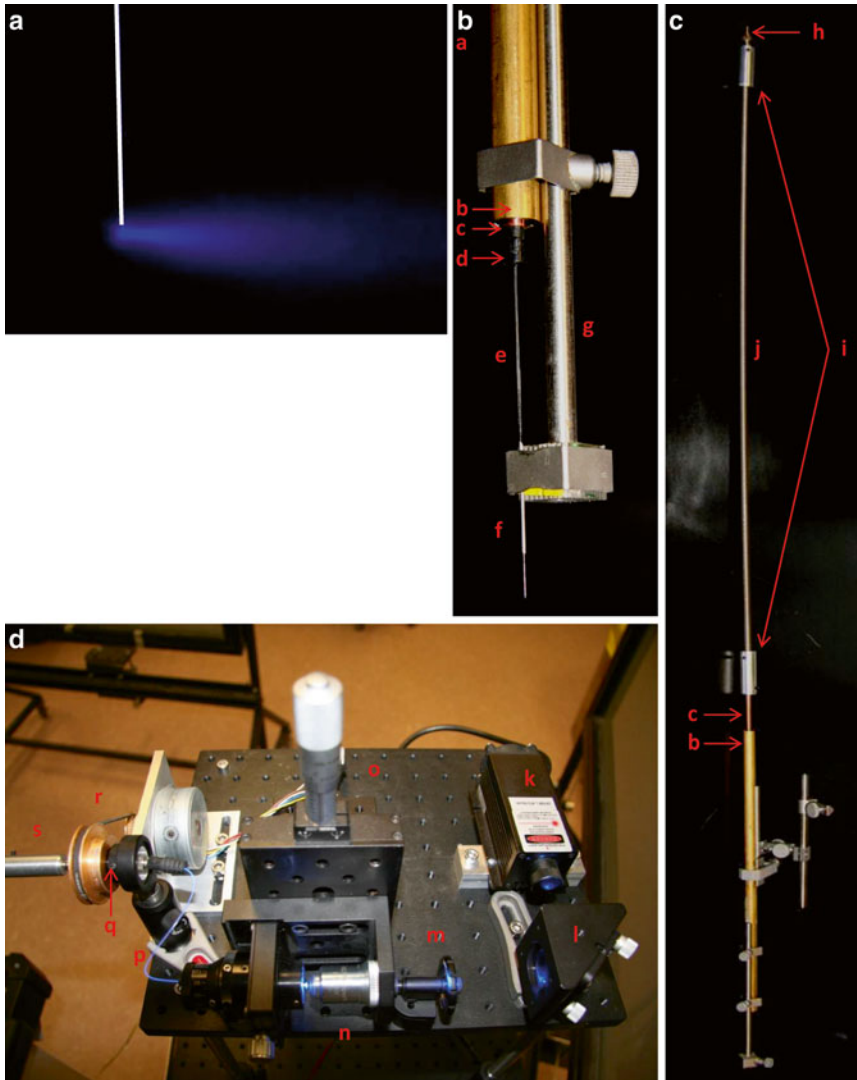


Fig. 1 Opto-mechanical setup. **(a)** Illumination pattern of the designed side-firing optical fiber. White bar indicates the fiber's position. **(b)** Tip of the freely rotating optical fiber. Brass guide tube is fixed to an electrode holder. Black plastic adaptor holds optical fiber in the center of the copper guide tube, which freely rotates in the brass guide tube with high-precision bearings (not visible). A 24G needle fixed on the electrode holder stabilizes rotation of the fiber. **(c)** Inner copper guide tube is linked to mono-coil tube, in which passes the optical fiber, terminated with SMA connector. **(d)** Laser coupling. Free laser beam is attenuated with an adjustable filter wheel and coupled in the optical fiber with a microscope objective. Kinematic mirror at 45° and X and Y micromanipulators allow precise adjustment of beam alignment. Stepper motor puts the rotary joint into motion via timing belt, to which the SMA connector in **(c)** is connected. *Component id.* a: large guide tube (brass), b: bearing (hidden), c: small guide tube (copper), d: cylindrical adaptors (plastic), e: optical fiber, f: 24G needle, g: microelectrode holder, h: SMA connector, i: homemade adaptors, j: mono-coil, k: laser source, l: mirror, m: attenuator, n: collimator, o: micromanipulator, p: optical fiber, q: rotary joint (hidden), r: gears and timing belt, s: top end of side-firing fiber. Figure adapted from [15]

adaptors and placing them at each end of the small guide tube, the optical fiber should rotate smoothly around its axis (Fig. 1b).

3. Fix a microelectrode holder to the end part of the outer metal guide tube and attach a 24G needle. Pass the exposed core of the optical fiber through the needle, which serves to stabilize the optical fiber while rotating (Fig. 1b, c).
4. The rotary joint allows for free rotation of the optical fiber. One side of the rotary joint (stator) should be fixed in place using a post. The other part of the rotary joint (rotor) is placed in a gearing.
5. The stepper motor and driver are used to rotate the rotary joint. Place the second gear on the shaft of the stepper motor and connect the two gears with the timing belt (Fig. 1d).
6. The mono-coil is a hollow flexible shaft that transmits rotary motion from the rotary joint to the guide tube. Fix one end of the mono-coil to the polished optical fiber connector and the other end to the metal guide tube with homemade adaptors (Fig. 1c).
7. Connect the optical fiber to the rotor of the rotary joint.

4.1.3 Laser Coupling

1. Fix laser source on breadboard (*see* Fig. 1d).
2. Place mirror with kinematic mirror mount at 45° with incident laser beam to deflect beam at right angle.
3. Place neutral density filter in the beam path. This will allow modulating output power of the fiber.
4. Fix collimator on an X and Y micromanipulator and direct laser beam in collimator.
5. Connect one end of the optical fiber to the collimator.
6. Using the mirror kinematic mount to make fine adjustments on the beam angle and the X and Y micromanipulators to precisely center the collimator on the beam, maximize light coming out of the connected optical fiber.
7. Connect the free end of the optical fiber to the stator of the rotary joint.

4.2 *In Vivo* Optogenetic Stimulation of Deep Brain Structures

In this study, mice expressing channelrhodopsin-2 (ChR2) fused to Yellow Fluorescent Protein under the control of the mouse thymus cell antigen 1 promoter were used (strain name: B6.Cg-Tg (Thy-COP4/EYFP), Jackson Laboratory). All procedures were carried out in accordance with the guidelines of the Canadian Council for the Protection of Animals and the experimental protocol was approved by the Ethics Committee of the Université de Montréal.

4.2.1 Animal Preparation

Mice were anesthetized with an intra peritoneal injection of urethane (2 g/kg). After testing reflexes on hind paw, 2 % Xylocaine® was injected subcutaneously in the region covering the trachea. The neck and the head of the mice was shaved and disinfected with iodine solution. Tracheotomy was performed in order to ease breathing.

The animal was then placed in stereotaxic frame. A flow of pure oxygen was directed toward the tracheal tube. Body temperature was maintained through the experiment at 38 °C with a heating pad and the electrocardiogram was continuously monitored (Fig. 2c).

Finally, the head of the mouse was stereotaxically aligned. Targeted brain structure, LGN, in mice is of very small size (<1 mm³). It is therefore of prime importance to have a precise stereotaxic alignment if we are to reach the LGN of the mice.

4.2.2 Reaching the Deep Brain Nucleus

To reach a deep brain structure with an optical fiber, one must first determine its exact stereotaxic position and find the best possible way to reach it. In this particular case, the LGN is situated directly under the primary visual cortex V1 (Fig. 2b) where we wish to image intrinsic optical signals. To avoid blocking access to V1, the optical fiber was inserted in the cortex with a 57° angle relative to the vertical. A small craniotomy (1 mm diameter) was performed with a micro drill (0.5 mm in diameter) at -2.3 mm relative to bregma in the sagittal axis and at 4 mm on the lateral axis.

To insure that the right location was found, a tungsten microelectrode was first used to record neural activity in the LGN (*see Note 2*). The microelectrode was fixed to the optical fiber stereotaxic holder (*see Subheading 4.1.2, step 3*). The microelectrode was then lowered through the bone opening and towards the LGN until robust visual multiunit responses were evoked by light flashes (approximately 2.7 mm from the surface) (troubleshooting, *see Note 3*).

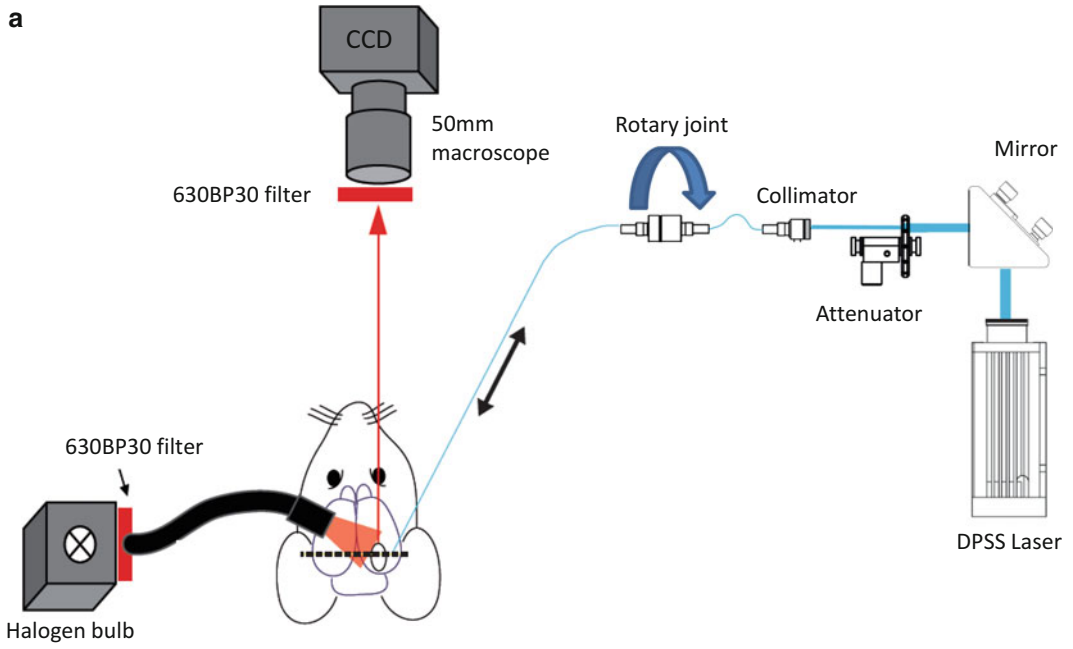
Once the localization of the LGN was confirmed, the microelectrode was removed and replaced by a 24G needle. The exposed core of the optical fiber was then passed through the needle, which served two purposes: first to maintain the same coordinates as the microelectrode and second to stabilize the optical fiber during its rotation. The optical fiber was then lowered in the brain at the same depth where visual responses were obtained, in order to optogenetically induce neuronal activity in the LGN.

4.2.3 Optogenetic Stimulation and Intrinsic Optical Imaging

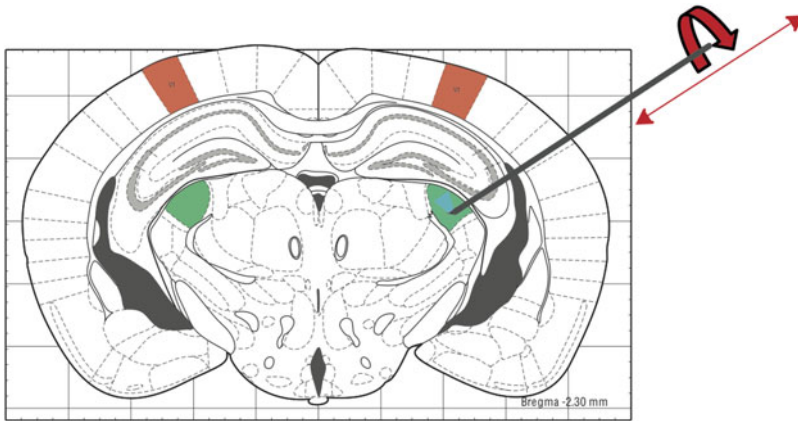
1. Intrinsic optical signals

The recording of neural activation was achieved with intrinsic optical imaging (IOI), which represents a powerful technique to visualize the global functional architecture of cortical areas in vivo. One approach is to monitor the slow

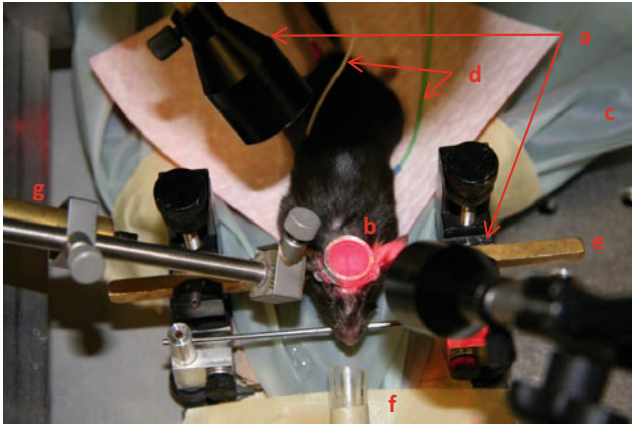
a



b



c



intrinsic changes in the optical properties of the active cortex over time. The main source for these activity-dependent intrinsic signals come from local variations in the concentration of deoxy- and oxy-hemoglobin within capillaries in response to the increased metabolic demand of active neurons [12]. The cortex was imaged directly through the skull by placing a circular ring above the visual cortex as an imaging chamber. The mouse skull is very thin and translucent, making intrinsic optical signals visible without the need for a craniotomy. The chamber was filled with agarose (1 %) and sealed with a coverslip to keep the skull hydrated and transparent.

A 12 bit CCD camera fitted with a macroscopic lens was used to record cortical activity. First, the brain was illuminated at 545 nm to image the cortical vasculature at high contrast in order to adjust the focus of the camera on the cortex. Light was guided from a filtered halogen bulb to the cortex using a fiber optic bundle (Fig. 2a). Intrinsic optical signals were acquired by illuminating the cortex with a 630 ± 15 nm light, a spectral band where absorption is sensitive to variations in deoxyhemoglobin concentration [13].

2. Stimulation and data acquisition

Precise control of fiber illumination conditions allowed us to define a finite volume of optogenetic activation. Single illumination pulses of 250 ms were used, a paradigm shown to be appropriate for the stimulation of channelrhodopsin 2 [14]. To limit the volumetric extent of excited neural tissue by light, the output power from the optical fiber tip was varied from 1 to 10 mW/mm²[15] (see Note 4).

Stimulus synchronization between optogenetic light pulse and IOI system was achieved using VDAQ software and Imager 3001 data acquisition hardware (Optical Imaging Ltd, Israel). Trials lasted a total of 20 s and camera frames were acquired at a rate of 4 Hz. A pre-stimulation period of 2 s preceded the continuous light pulse stimulation of 250 ms, followed by a post-stimulation period of 18 s, during which the slow hemodynamic response occurred. Each trial was repeated 20 times for any given radial or axial position of the fiber.

Fig. 2 Experimental setup. (a) Simplified experimental design. A halogen bulb with a 630BP60 filter is used for illumination in order to measure intrinsic signal from the cortex with a CCD camera placed over the head. Side-firing optical fiber is lowered in the LGN by triangulation, where it is free to rotate and slide along its axis. (b) Coronal slice of the *dashed line* in (a). Adapted from Franklin and Paxinos, 2013 [17]. Fiber is inserted at an angle of 57° through a small craniotomy into the lateral geniculate nucleus (*green* region) using a stereotaxic holder (not shown). Primary visual cortex is presented in *red*. (c) Animal preparation. Fiber bundles guide red light to shine the cortex, through an agarose-filled chamber. Optical fiber is inserted lateral to the chamber. Mouse head is fixed with ear bars. *Component id.* a: fiber optic bundle, b: imaging chamber, c: heating pad, d: ECG electrodes, e: ear bars, f: oxygen flow, g: side-firing optical fiber

5 Typical Results

1. Electrophysiological recording in the LGN

A tungsten microelectrode is used to confirm the position of the lateral geniculate nucleus. Figure 3a shows a typical recording of multiunit responses in the LGN evoked by visual stimuli (flash).

2. IOI following optogenetic stimulation of LGN

Hemodynamic responses are slow compared to neural activity, lasting 4–10 s, with maximal signal variation occurring approximately 2–3 s after neural stimulation. Figure 3b shows signal variation between camera frame acquired 2.5 s after optogenetic stimulation and pre-stimulation condition (0–2 s) over primary visual cortex ipsilateral to stimulated LGN, over 20 trials. A neural activation is characterized by a drop of reflectance signal, as shown in blue. By averaging the signal in a region of the primary visual cortex (square region in Fig. 3b) and subtracting control trials, we can visualize signal variation over time to obtain the hemodynamic response time course over 20 trials (Fig. 3c). We see a rapid loss of signal at time $t=0$ s where optogenetic stimulation occurs, followed by a progressive rise of reflectance, characteristic of a hemodynamic response.

To have an insight on the spatial extent of optogenetic stimulation in the LGN, the visual cortex area consequently activated was measured. A Student t test indicated areas having a significant reflectance difference between peak activation (2.5 s after stimulation) and baseline (pre-stimulation average), thus delimiting a precise activation zone, as presented in Fig. 3d.

The activation map presented in Fig. 3d is for a precise position of the optical fiber in the LGN of a mouse. By rotating the fiber around its axis, varying its depth and by modulating the output power of the fiber, it is possible to activate different neuron populations, giving rise to different activation maps in primary visual cortex. *For further investigation using the present setup for LGN optogenetic activation, please consult [15].*

6 Notes

1. Bearing and guide tube fitting

Fitting the bearings firmly in the metal guide tubes may reveal to be challenging. If the inner metal guide is too big to fit in the bearing, try sanding or cooling the metal guide tube to reduce its diameter to fit in the bearing. Also, for fitting the bearing in the larger guide tube, heating the rod will temporarily expand the tube to give a little wiggle room. Teflon can be used to tighten any loose fits.

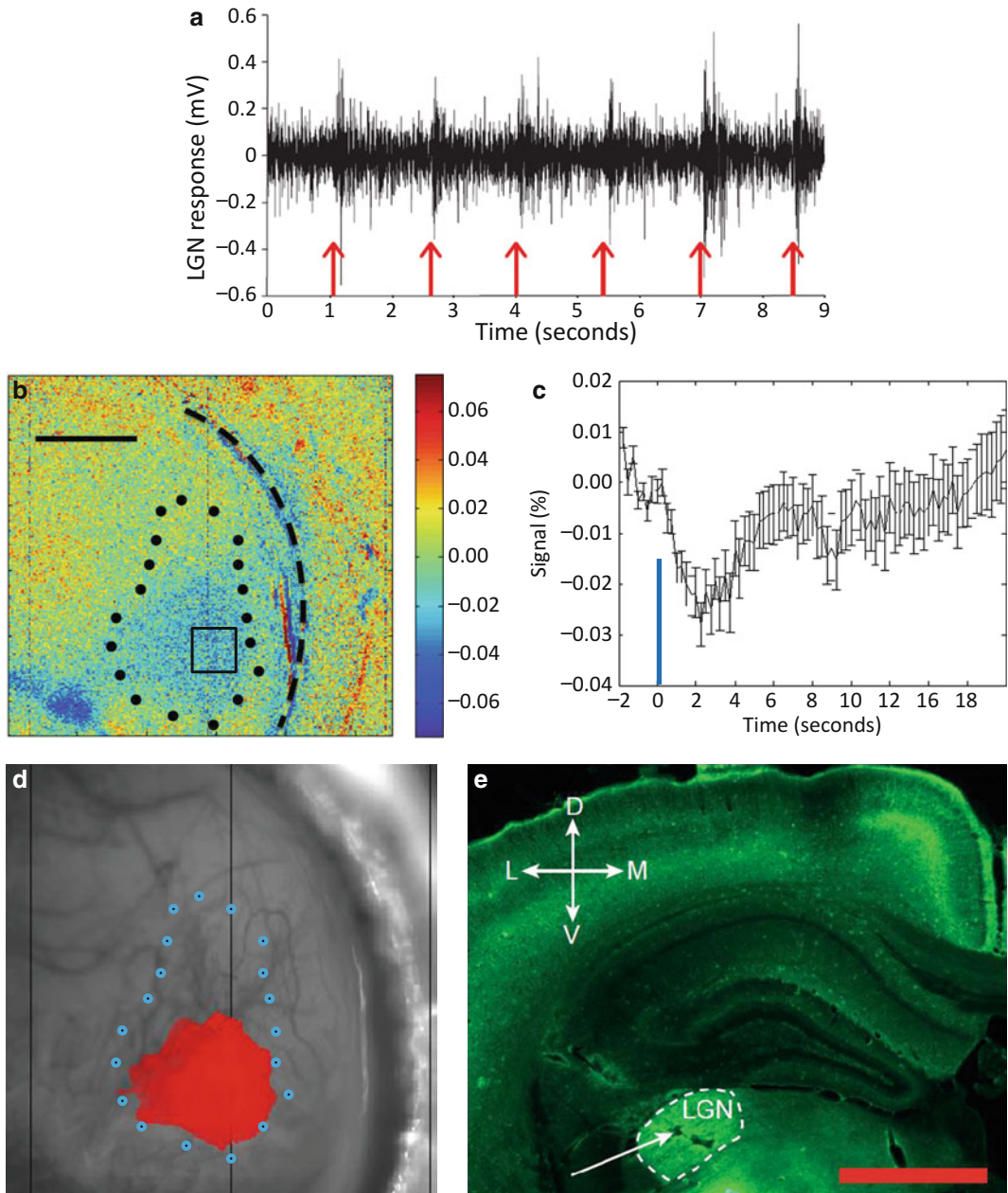


Fig. 3 In vivo optogenetic stimulation and IOI recordings. **(a)** Extracellular multiunit recordings in the LGN in response to visual stimuli (*red arrows*) (adapted from [15]). **(b)** Reflectance signal variation on cortical surface, 2.5 s following optogenetic stimulation of the LGN. Boundaries of primary visual cortex are delimited with *dots*, whereas *dashed line* indicates edge of imaging chamber. Color code represents signal variations in percentage. Optical power at fiber tip: 3,2 mW/mm². Scale bar: 1 mm. **(c)** Time course of relative reflectance signal variations (in %) for the region identified by a *square* in **(b)**, averaged over 20 trials. Light pulse duration is represented in *blue*. Error bars show the standard error. **(d)** Activation map in **(b)** after delimitation with a Student *t* test ($\alpha = 0.01$) superimposed on the anatomical image of mouse cortex. Boundaries of primary visual cortex are delimited with *dots*. **(e)** Immunofluorescence image of ChR2 expression from coronal brain section taken at the level of the LGN, delimited by *dashed line* (adapted from [15]). The optical fiber insertion path is indicated by the *arrow*. Dorsoventral (D–V) and mediolateral (M–L) axes are presented. Scale bar: 1 mm. Figure adapted from [15]

2. Optrode

In this protocol, an electrode is used to first confirm the right stereotaxic alignment for the optical fiber. Optrodes are now being developed and commercialized [7, 16], which could be used in this protocol for both recording electrical activity and optogenetic stimulation.

3. Difficulty reaching deep brain structures

Reaching the LGN can be quite difficult due to its small size (<1 mm³). Precise stereotaxic alignment of the brain is of prime importance. Make sure that the Lambda and Bregma intersection points [17] are at the same height and in a straight line on the mediolateral axis. If the deep brain structure is not reached from the first descent of the electrode, remove and insert it at a distance equivalent to the diameter of the structure from the initial entry point. Continue insertions around the initial entry coordinates in a grid pattern until recordings from the desired structure are obtained.

4. Monte Carlo simulation

To evaluate the volumetric extent of optogenetic stimulation in deep brain structures, our group has used Monte Carlo simulation [18]. Based on estimated tissue optical properties, such simulations allow users to estimate the volume of excited tissues by various output power of the fiber [15].

Acknowledgment

Supported by a Fonds de Recherche du Québec-Nature et Technologies (FRQ-NT) grant #165075 (Projet de recherche en équipe) to F.L. and C.C. and by Natural Sciences and Engineering Research Council of Canada (NSERC) grants #194670 and 239876 to C.C. and F.L., respectively. A.C. was supported in part by scholarships from the Fonds de Recherche en Santé du Québec (FRSQ) vision network and the Faculté des Études Supérieures et Postdoctorales-Institut de Génie Biomedical (FESP-IGB) of the Université de Montréal.

References

1. Berman RA, Wurtz RH (2008) Exploring the pulvinar path to visual cortex. *Prog Brain Res* 171:467–473, Elsevier
2. Boyden ES, Zhang F, Bamberg E et al (2005) Millisecond-timescale, genetically targeted optical control of neural activity. *Nat Neurosci* 8:1263–1268
3. Scott NA, Murphy TH (2012) Hemodynamic responses evoked by neuronal stimulation via channelrhodopsin-2 can be independent of intracortical glutamatergic synaptic transmission. *PLoS One* 7:e29859
4. Mateo C, Avermann M, Gentet LJ et al (2011) In vivo optogenetic stimulation of neocortical excitatory neurons drives brain-state-dependent inhibition. *Curr Biol* 21:1593–1602
5. Yizhar O, Fenno LE, Prigge M et al (2011) Neocortical excitation/inhibition balance in information processing and social dysfunction. *Nature* 477:171–178

6. Fodor L, Ullmann Y, Elman M (2011) Light tissue interactions. In: Aesthetic applications of intense pulsed light. Springer, London
7. LeChasseur Y, Dufour S, Lavertu G et al (2011) A microprobe for parallel optical and electrical recordings from single neurons *in vivo*. *Nat Methods* 8:319–325
8. Zorzos AN, Scholvin J, Boyden ES, Fonstad CG (2012) Three-dimensional multiwaveguide probe array for light delivery to distributed brain circuits. *Opt Lett* 37:4841
9. Fenno L, Yizhar O, Deisseroth K (2011) The development and application of optogenetics. *Annu Rev Neurosci* 34:389–412
10. Chalupa L, Williams R (2008) Eye, retina and visual system of the mouse. The MIT Press, Cambridge
11. Grinvald A, Lieke E, Frostig RD et al (1986) Functional architecture of cortex revealed by optical imaging of intrinsic signals. *Nature* 324:361–364
12. Hillman EMC (2007) Optical brain imaging *in vivo*: techniques and applications from animal to man. *J Biomed Opt* 12:051402
13. Frostig RD, Masino SA, Kwon MC, Chen CH (1995) Using light to probe the brain: intrinsic signal optical imaging. *Int J Imaging Syst Technol* 6:216–224
14. Wang J, Wagner F, Borton DA et al (2012) Integrated device for combined optical neuro-modulation and electrical recording for chronic *in vivo* applications. *J Neural Eng* 9:016001
15. Castonguay A, Thomas S, Lesage F, Casanova C (2014) Repetitive and retinotopically restricted activation of the dorsal lateral geniculate nucleus with optogenetics. *PLoS One* 9:e94633
16. Lin S-T, Gheewala M, Wolfe JC, et al (2011) A flexible optrode for deep brain neurophotonics. Paper presented at the 5th International IEEE EMBS Conference on Neural Engineering, Cancun, April 27–May 1 2011
17. Franklin KBJ (2013) Paxinos and Franklin's: the mouse brain in stereotaxic coordinates, 4th edn. Academic, Amsterdam, An imprint of Elsevier
18. Boas D, Culver J, Stott J, Dunn A (2002) Three dimensional Monte Carlo code for photon migration through complex heterogeneous media including the adult human head. *Opt Express* 10:159–170